ANTIOXIDANTS & REDOX SIGNALING
Volume 11, Number 1, 2009

DOI: 10.1089/ars.2008.2150

Original Research Communication

Oral Administration of Blueberry Inhibits Angiogenic Tumor Growth and Enhances Survival of Mice with Endothelial Cell Neoplasm

Gayle Gordillo,[1,2] Huiqing Fang,[1] Savita Khanna,[2] Justin Harper, Gary Phillips,[3] and Chandan K. Sen[2]

Abstract

Endothelial cell neoplasms are the most common soft tissue tumor in infants. Subcutaneous injection of spontaneously transformed murine endothelial (EOMA) cells results in development of hemangioendothelioma (HE). We have previously shown that blueberry extract (BBE) treatment of EOMA cells *in vitro* prior to injection *in vivo* can significantly inhibit the incidence and size of developing HE. In this study, we sought to determine whether oral BBE could be effective in managing HE and to investigate the mechanisms through which BBE exerts its effects on endothelial cells. A dose-dependent decrease in HE tumor size was observed in mice receiving daily oral gavage feeds of BBE. Kaplan–Meier survival curve showed significantly enhanced survival for mice with HE tumors given BBE, compared to control. BBE treatment of EOMA cells inhibited both c-Jun N-terminal kinase (JNK) and NF-κB signaling pathways that culminate in monocyte chemoattractant protein-1 (MCP-1) expression required for HE development. Antiangiogenic effects of BBE on EOMA cells included decreased proliferation by BrdU assay, decreased sprouting on Matrigel, and decreased transwell migration. Thus, this work provides first evidence demonstrating that BBE can limit tumor formation through antiangiogenic effects and inhibition of JNK and NF-κB signaling pathways. Oral administration of BBE represents a potential therapeutic antiangiogenic strategy for treating endothelial cell neoplasms in children. *Antioxid Redox Signal* 11, 47–58.

Introduction

Endothelial cell neoplasms are the most common soft tissue tumor in infants, affecting 3–10% of all infants (13, 37, 39). Approximately 10% of these lesions will threaten the well-being of the child by obstructing vital structures, and 1% of these lesions threaten the life of the child (39). Current treatment options for endothelial cell neoplasms are high dose steroids and if those fail, then interferon therapy. Both of these treatment options are immunosuppressive and have extremely high risk side effect profiles. These risks include opportunistic infection, gastric ulcers, femur fractures, delays in achieving developmental milestones, and for interferon therapy the risk of spastic diplegia, a global neurologic insult that may not be reversible. Surgery is usually not a good option because of the risk of life-threatening blood loss or significant residual deformity as the results of tumor removal. Thus, the treatment can be as threatening to the child as the disease. The majority of these lesions occur in the head and neck area, and the lack of safe therapeutic alternatives means that many children and their parents are forced to accept the physical deformity that comes with it.

Treatment of endothelial cell neoplasms with a nutritional approach is appealing because of the young age of the patient population and the inherent safety of using food products. It may also provide an opportunity for treatment to children who have a physical deformity, but do not have their life threatened by the lesion. Extracts from fruits and plants have been investigated for use in treating many diseases because the polyphenol chemical structure of flavonoids and their derivative products, such as anthocyanins, which provide the pigment and coloration of plants

[1]Division of Plastic Surgery and [2]Laboratory of Molecular Medicine, Department of Surgery, Davis Heart Lung Research Institute, and [3]Center for Biostatistics, The Ohio State University, Columbus, Ohio.

and berries, have potent antioxidant and anti-inflammatory properties (65). These qualities translate into an ability to alter host response to viruses (27), cancer (24), and a wide range of inflammatory insults (46, 54). For example, grape seed extract has been used to protect mouse hearts against ischemia reperfusion injury (41), and sour cherry flavonoids can protect retinas against ischemia reperfusion injury (59). Blueberry extract (BBE) has been shown to have antiangiogenic and antioxidant properties that may be beneficial for treating endothelial cell neoplasm (47).

Using a validated murine model of endothelial cell neoplasm, our group has previously shown that pretreatment of neoplastic endothelial (EOMA) cells with blueberry extract *in vitro*, prior to injecting these cells into mice, can decrease the incidence and size of tumors by over 50% (3). To follow up on those encouraging results, we wanted to test a more clinically relevant model of BBE delivery to prepare for possible clinical trials. Specifically, we sought to determine whether oral administration of BBE could be effective as a dietary intervention for endothelial neoplasms in children. We also sought to gain greater insight into the mechanisms behind the effects of BBE on endothelial cell neoplasms.

The murine model used for this study was first described in 1971 (20). The endothelial cell phenotype of EOMA cells has been confirmed (38, 50), and other investigators have used it to test antiangiogenic compounds for tumor therapy (1, 28, 37, 60, 62). When EOMA cells are injected subcutaneously into mice, they form hemangioendotheliomas (HE) with 100% efficiency. These tumors have been shown to closely mimic the human condition. Mice injected with EOMA cells develop Kassabach–Merritt syndrome, a key diagnostic feature of HE in humans that is characterized by progressive sequestration of red blood cells and platelets in the tumor (20, 64). As the tumors become engorged with blood and platelets, anemia and bleeding problems ensue and are the ultimate cause of death in both humans and mice.

Another critical feature the EOMA model has in common with human neoplasms is the expression of monocyte chemoattractant protein-1 (MCP-1). The most common form of human endothelial cell neoplasm, the infantile hemangioma, has been shown to have MCP-1 expression that occurs only during tumor proliferation (23). Several other human tumors, including breast (51, 61), bladder (2), and ovarian cancer (18), have also express MCP-1, and the prognosis for breast cancer patients correlates inversely with MCP-1 expression levels (*e.g.*, the higher the MCP-1 levels the poorer the prognosis) (29, 61). We have shown that MCP-1 produced by EOMA cells is required for HE tumorigenesis (14) and that expression of MCP-1 from EOMA cells is subject to redox control (15). Given the critical role of MCP-1 in promoting the development of HE and potentially important role it has for other human tumors, we wanted to investigate the effects of BBE on signaling events that regulate MCP-1 expression.

The MCP-1 promoter contains binding sites for the nuclear transcription factors activator protein-1 (AP-1) and nuclear factor kappa-B (NF-κB) (34, 57). Both these transcription factors are implicated in tumorigenesis. Experiments were performed to determine whether BBE can inhibit the NF-κB and the mitogen activated protein kinase (MAPK) signaling pathway of JNK, c-Jun, and AP-1, which culminates in MCP-1 expression. Both of these signaling pathways have also been shown to be induced by oxidant signals (7, 33, 40, 58). Therefore, the antioxidant properties of BBE *in vivo* was also addressed. Results reported in this work demonstrate that oral BBE can inhibit specific molecular mechanisms that promote tumorigenesis, and provide further evidence to support the pursuit of BBE as a potential nutritional intervention for endothelial cell neoplasms in children.

Materials and Methods

Blueberry extract

Standardized blueberry extract was obtained from Inter-Health Nutraceuticals, Inc. (Benicia, CA). In brief, blueberries were subjected to a water/ethanol extraction and the extract was then freeze-dried and ground into a fine powder. We previously reported a complete quantitative profile of the flavonoid components present in BBE and its antioxidant capabilities as measured by the oxygen radical absorbance capacity (ORAC) (47).

EOMA cell culture

Cell culture was done as previously described (15). Briefly, EOMA cells (gift from C. Orosz, Ph.D, also available at www.attc.org) were maintained in DMEM supplemented with 10% fetal calf serum (FCS) and 1% penicillin/streptomycin and incubated at 37°C and 5% CO_2, which constitutes normal growth media (NGM). All experiments investigating the signal transduction pathway cells were performed in low serum media (LSM) consisting of DMEM + 0.5% FCS +1% penicillin/streptomycin to avoid serum response element activation. BBE was suspended in 100% DMSO to generate a stock solution (50 mg/ml). For all *in vitro* BBE treatments, this stock solution was added to LSM, so that the final concentration of BBE was 150 μg/ml and the final concentration of DMSO was 0.3%. The same concentration of DMSO (0.3%) served as the vehicle control for all *in vitro* experiments.

In vivo *experiments*

Mice were fed standard chow and water ad libitum and housed in clean environments in compliance with Institutional Laboratory Animal Care and Use Committee guidelines of The Ohio State University. Female 129P/3 mice (Jackson Laboratories, Bar Harbor, ME) between 6–8 weeks of age and weighing 15–20 g received subcutaneous injection of EOMA cells, as previously described (15). Serum samples were obtained by retro-orbital bleed prior to EOMA cell injection to determine baseline oxidative measurements. Gavage feeding of blueberry extract suspended in sterilized double distilled H2O at the doses indicated in respective figure legends was initiated the day of injection and continued once a day. Control mice were gavage fed the same volume (150 μl) of sterilized double distilled H2O. For experiments to determine tumor volume, mice were euthanized on postinjection day 7, and tumor specimens and blood samples were collected. Tumor volume was determined using calipers to measure length $\times$ width $\times$ height of each tumor. For the survival studies, mice received a once daily gavage feed of either sterilized double distilled H2O (vehicle control) or BBE at 20 mg/kg beginning the day of EOMA cell injection. The death rate was calculated for each group over a 30-day period.

Thiobarbituric acid reactive substances (TBARS) assay

TBARS assay was performed according to the manufacturer's instructions (Zeptometrix, Buffalo, NY). Blood collected at the time of necropsy was incubated at room temp for 30 min to form clots, then spun at 3,500 rpm × 10 min. The serum/supernatant collected was either assayed immediately or frozen at −80°C. The malondialdehyde (MDA) standard curve was generated according to the manufacturer's instructions, and a 100 μl aliquot of each standard (run in duplicate) was placed in a 96-well plate. A 25 μl serum aliquot was added to a reaction mixture containing TBA in a 12 × 75 mm disposable glass culture tube, mixed by swirling, incubated at 95°C for 60 min, cooled on ice for 10 min to reach room temperature, then centrifuged at 3000 rpm × 15 min. A 100 μl aliquot of this reaction mixture was added to separate wells in a 96-well plate that also contained the MDA standard curve. Fluorescence was detected using a Bio-TEK ELX 808IU microplate reader set at 530 nm excitation and 590 nm emission with a gain of 50.

HPLC detection of oxidized and reduced glutathione

Whole blood samples in 200 μl aliquots were frozen in liquid nitrogen immediately after collection at the time of necropsy. Sample preparation, mobile phase, and column used for glutathione assay were as previously described (53). A 5 μl aliquot of the sample solution prepared for HPLC analysis was used for protein quantitation using the Quanti-iT Protein Assay kit (Invitrogen, Carlsbad, CA). Glutathione (GSH) was detected in mouse blood using an HPLC-coulometric electrode array detector (Coularray Detector, model 5600 with 12 channels; ESA Inc., Chelmsford, MA) (48). This system uses multiple channels with different redox potentials. Applied potentials started at 300 mV and were analyzed up to 800 mV in 100 mV increments. Signals from channels set at 700 mV were used for quantification of GSH and signals from 800 mV were used for quantification of GSSG.

Cytotoxicity assay

EOMA cells in NGM were seeded in flat bottom 96-well culture plates at 6,000 cells/well and incubated at 37°C and 5% CO_2 for 6 h. The media was changed to LSM and BBE treatments and 0.3% DMSO (vehicle) controls at the indicated concentrations were added at the same time. The cells were incubated for 24 h, followed by LDH assay using the TOX-7 *in vitro* toxicology kit (Sigma, St. Louis, MO), according to the manufacturer's instructions. LDH absorbance was measured at 490 nm using the Bio-TEK ELX 808IU micro plate reader (Bio-TEK INSTRUMENTS, INC, Winooski, VT). Total LDH for each sample was calculated by adding LDH values from cell supernatants + pelleted cell lysates. LDH leakage calculated as LDH cell supernatant/total LDH.

JNK assay

EOMA cells were seeded using NGM at 8000 cells/well (8×10^4 cells/ml) in a 96-well plate. After 8 h incubation at 37ºC and 5% CO_2, NGM was replaced with LSM and 150 μg/ml of BBE was then treated followed by overnight incubation. After BBE pretreatment, cells were activated for 15 min with either tumor necrosis factor-alpha (TNF-α) 400 IU/ml (R & D Systems, Minneapolis, MN) or the JNK inhibitor SP600125 at 30 μ*M* (Calbiochem, San Diego, CA). Cells were fixed with 4% formaldehyde in PBS to stop the reactions. JNK phosphorylation was detected using the Cellular Activation of Signaling Elisa (CASE Kit, SuperArray Bioscience Corp., Frederick , MD), according to the manufacturer's instructions. There are two different primary antibodies with this kit: one monoclonal antibody detects only phosphorylated (activated) JNK, and the other detects total JNK. After the primary and secondary antibody reaction, the developing solution and stop solutions were added. Absorbance was measured at 450 nm to detect either total or phosphorylated JNK. The relative number of cells in each well was quantified by washing the cells and adding a colorimetric cell staining buffer according to the manufacturer's instruction and measuring absorbance at 595 nm. Results for each sample are reported as a ratio of antibody absorbance versus protein absorbance (OD450:OD595) to standardize samples against relative cell number. The relative extent of JNK phosphorylation for each sample was reported as the OD450:OD595 for phosphorylated JNK versus OD450:OD595 for total JNK.

c-Jun assay

This was performed using an ELISA-based kit (Active Motif, Carlsbad, CA). EOMA cells were plated in 100 mm tissue culture dishes at 2×10^6 cells/plate in 10 ml NGM. After 6 h, the media was changed to 10 ml LSM, and the BBE (150 μg/ml) treatments added. Cells were incubated in LSM with BBE for 36 h at 37° C and 5% CO_2. A vehicle control consisting of 0.3% DMSO was included in the experimental design. After BBE pretreatment, EOMA cells were stimulated with TNF-α (400 IU/ml) for 1 h. Cells were harvested by scraping and nuclear protein extracted according to the manufacturer's instructions. Nuclear extract was quantified using the DC protein reagent kit (Bio-Rad Hercules, CA). A 2 μg aliquot of nuclear extract was placed in the wells of a 96-well plate that had the bottom coated with a consensus binding oligonulceotide for AP-1 (TPA-response element (TRE) 5′-TGAGTCA-3′). The primary antibody detected activated/phosphorylated cJun by recognizing an epitope on cJun that is accessible only upon DNA binding. A horseradish peroxidase conjugated secondary antibody was used for colorimetric detection of the bound primary antibody. Wild-type consensus oligonucleotide that competes for the AP-1 binding site was used as a control to confirm the specificity of the assay (data not shown). Absorbance at 450 nm was used for detection.

AP-1 luciferase plasmid preparation

The pAP-1 luc plasmid (Stratagene, Cedar Creek, TX) containing a luciferase reporter gene and an ampicillin-resistance gene was amplified in DH5-α E. coli cells (Invitrogen) by placing 0.5 μl of pAP-1 luc plasmid (1 μg/ul in Tris-EDTA buffer) in 40 μl of DH5-α stock solution on ice and incubating for 30 min. The reaction mixture was heated in a 42°C water bath for 45 sec and immediately placed back on ice for 2 min. S.O.C. transformation media (Invitrogen; 1 ml) was added to the reaction mixture, which was then transferred to a 15 ml tube and incubated at 37°C for 1 h. A 50 μl aliquot of transfected DH5-α cells was plated onto 1.5% agar plates made with LB media and ampicillin (100 μg/ml) and

incubated at 37°C for 16 h. Single colonies were selected from the plate, inoculated in 1 ml of LB media and incubated at 37°C for 16 h. A 200 μl aliquot of this mixture was added to 100 ml of LB media and incubated at 37°C for 16 h. Plasmids were purified from this mixture using a midiprep system (Gibco BRL, Carlsbad, CA).

AP-1 luciferase assay

EOMA cells were seeded in 12-well plates at 1×10^5 cells/well in NGM and incubated at 37°C and 5% CO_2 for 6 h. The media was changed to LSM with the BBE treatments added as described for the c-Jun assay above. The cells were incubated in LSM with BBE at 37°C and 5% CO_2 for 16 h and then transfected with an AP-1 luciferase plasmid (Stratagene, Cedar Creek, TX) using Lipofectamine 2000 (Invitrogen). Reaction mixture 1 consisted of 100 μl Opti-MEM (Gibco, Carlsbad, CA) + 0.5 μg AP-1 plasmid per well, and reaction mixture 2 consisted of 100 μl Opti-MEM + 3 μl Lipofectamine per well allowed to incubate at room temperature for 5 min. Reaction mixtures 1 and 2 were added together and incubated at room temp for 30 min. The cell culture media was changed to 200 μl/well of the combined reaction mixtures + 500 μl/well of DMEM +0.5% FCS. The cells were incubated in this transfection media for 2.5 h at 37°C and 5% CO_2. They were washed twice with DMEM and then incubated in 1 ml of LSM with BBE for 36 h. Cells were then challenged with TNF-α at 400 IU/ml. After 1 h, cells were washed twice with PBS. Lysis buffer (Promega, San Luis Obispo, CA) was added at 0.2 ml per well and incubated on a rocker for 15 min at room temperature. Next, cells were collected by scraping and placed in a microfuge tube on ice. Samples were vortexed for 10–15 sec, then spun at 12,000 $g \times 15$ sec at room temperature. The supernatants were collected and a Bio-Rad protein assay (Bio-Rad) performed on a 10 μl aliquot. In a round-bottom 5 ml polystyrene tube (Sarstedt, Newton, NC), 10 μl of cell lysate was mixed with 100 μl of RT 1× luciferase assay reagent (Stratagene). Light emission was detected using a Lumat LB 9507 luminometer (Berthold Technologies, Oak Ridge, TN) with a 2 sec measuring interval and a 10–30 sec integration time. Results were standardized as relative light units per mg protein.

MCP-1 ELISA

EOMA cells were seeded in 12-well plates at 8×10^4 cells/well in NGM and incubated at 37°C and 5% CO_2 for 5–8 h. The media was changed to LSM with BBE treatments added and the cells incubated overnight. Cells were then challenged with TNF-α at 400 IU/ml for 2 h, and the supernatants and cell lysates were both collected. Cell lysates were prepared as previously described (15). MCP-1 ELISA was performed on cell supernatants using the CCL2/JE/MCP-1 Quantikine ELISA kit (R&D Systems, Minneapolis, MN). Absorbance was detected at 450 nm. Bio-Rad protein assay was performed on an aliquot of all tested samples and results standardized per mg protein.

NF-κB activation

This assay was performed using an ELISA-based kit (Active Motif, Carlsbad, CA) similar to the one used to measure c-Jun activation. The method used was the same as that followed for c-Jun except for the following: (a) 10 μg of nuclear extract was applied per well; (b) pyrollidine dithiocarbamate (PDTC) (Sigma, St. Louis, MO) was used as an inhibitor of NF-κB at 200 μM and was applied to the cells at the same time as the BBE treatment, and (c) TNF-α (400 IU/ml) treatment was only for 15 min. The NF-κB consensus binding oligonucleotide coated on the bottom of each well was 5′-GGGACTTTCC-3′.

BrdU assay

EOMA cells were seeded in 100 μl NGM contained in flat-bottom 96-well culture plates at 3,000 cells/well and incubated overnight. The media was changed to LSM and treatments consisting of BBE (150 μg/ml), or SP600125 (30 μM) were also added at this time. The cells were incubated for 6 h. Next BrdU labeling solution, included as part of a cell proliferation ELISA (BrdU) kit (Roche, Indianapolis, IN), was diluted 1:100 in LSM and 10 μl was added to each well. Cells were incubated overnight at 37°C and 5% CO_2. ELISA based BrdU assay was performed according to the manufacturer's instructions. Once the colorimetric substrate was added, incubation was kept to < 5 min and absorbance read at 450 nm, using a Bio-TEK ELX 808IU microplate reader.

Matrigel angiogenesis assay

EOMA cells were seeded in 2 ml NGM at 2.5×10^5 cells/ml using 300 mm plates (Falcon, Franklin Lakes, NJ). Cells were incubated at 37°C and 5% CO_2 for 6 h. The media was changed to LSM with BBE treatments added at this time and cells incubated overnight. Cells were trypsinized, resuspended in LSM at 6×10^4 cells/ml and 500 μl of cell suspension seeded on growth factor reduced, phenol red free Matrigel (BD Biosciences, Bedford, MA) prepared according to the manufacturer's instructions in 4-well tissue culture plates (Nunc, Rochester, NY). BBE (150 μg/ml), SP600125 (30 μM) and vehicle control (0.3% vol/vol DMSO) treatments were added at the time of cell seeding on Matrigel and incubated at 37°C and 5% CO_2 overnight. Cell cytoplasms were fluorescently stained by adding 0.5 μl of Calcein AM (Invitrogen; 8.3 μg/μl DMSO) to each well and incubating at 37°C and 5% CO_2 for 15–60 min. Cells were washed with PBS and the nuclei stained by adding 1 μl of DAPI (Invitrogen) in 2 ml of PBS to each well. Fluorescent images were obtained immediately using a Zeiss Axiovert 200M microscope. Tube formation was quantified by examining at least three images per well using AxioVision LE software version 3.1 (Zeiss, Munich, Germany) to measure total area within the tubes for a standard 50X magnification image.

Transwell assay

Transwell inserts with 8-μm pore size (Costar, Corning, NY) were equilibrated by incubation in LSM overnight at 37°C and 5% CO_2 placed in the 24-well plates. EOMA cells were pretreated with 150 μg/ml of BBE or 0.3% DMSO for the vehicle control and incubated overnight in LSM at 37°C and 5% CO_2. EOMA cells were trypsinized and a 100 μl aliquot (10^5 cells/100 μl LSM) placed in the upper chamber. Cells were treated with either 150 μg/ml of BBE, JNK inhibitor SP600125 (30 μM), or 0.3% DMSO for the vehicle control at the time of seeding in the upper well. NGM (0.6 ml)

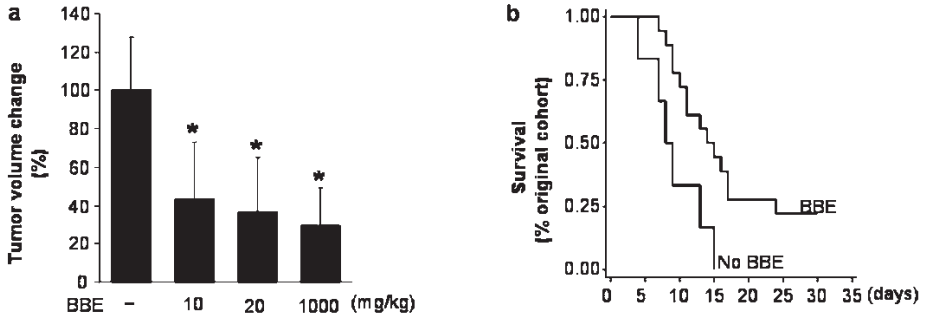

FIG. 1. Oral administration of BBE decreases HE tumor growth *in vivo* and prolongs survival. (**a**) Female 129 P/3 mice ($n = 6$ per group) injected with EOMA cells were treated with a daily oral gavage feeding of vehicle control (ddH_2O) or BBE at the doses indicated starting immediately after EOMA cell injection. Tumor specimens were collected 7 days after EOMA cell injection, and volume determined using caliper measurements (length × width × height). Tumor volume was significantly decreased in all BBE treated mice compared to vehicle fed controls (mean ± SD; $^{**}p < 0.01$ ANOVA); (**b**) Effects of BBE on survival was compared between mice treated with oral BBE at 20 mg/kg ($n = 18$) *versus* vehicle control ($n = 6$). Kaplan–Meier survival curve shows a significant increase in survival time for mice receiving BBE compared to those given vehicle control ($p < 0.02$ log-rank analysis).

was added into lower chamber at the time of cell seeding in the upper chamber. The cells were incubated for 5 h at 37°C and 5% CO_2, rinsed with PBS, then fixed with 10% formalin for 10 min. Cell nuclei were stained with DAPI (1:10,000) and fluorescent images of the lower surface of the transwell membrane obtained using a Zeiss Axiovert 200M microscope. Quantitation was done by counting the number of cells observed in each image divided by the total area (2.4 mm^2) to calculate EOMA cells per mm^2. There were three images quantified per membrane.

Statistical methods

One-way analysis of variance (ANOVA) was used to test the treatment differences on the response variable for all data except for Fig. 1. If the ANOVA F-test was statistically significant (p value < 0.05) then a post hoc analysis with the Holm's method was used to test prespecified treatment levels. The Holm's method was used to control the overall type I error involved in multiple testing within each analysis. For Fig. 1a, linear regression was used to test if tumor volume was associated with treatment dose. Log-rank analysis was used to evaluate results of the Kaplan–Meier survival curve in Fig. 1b. All bar graphs represent the mean value with the error bars indicating one standard deviation from the mean. These analyses were run using Stata, version 9.2, Stata Corporation, College Station, Texas.

Results

The effects of oral administration of BBE on tumor development and mouse survival was studied in 6- to 8-week-old female129P/3 mice injected subcutaneously with EOMA cells. The mice received daily gavage feeds of either vehicle control (sterilized ddH2O) or BBE at the indicated doses. Tumor size is an important indicator of HE lethality because it is the sequestration of blood and platelets within the tumor that causes the death of the affected mice. These tumors do not metastasize. With a single daily administration of oral BBE, there was a dose-dependent decrease in the size of the tumors that did develop in BBE treated versus vehicle control fed mice. This observation reached statistical significance beginning with BBE doses as low as 10 mg/kg/day (Fig. 1A). The dose of 20 mg/kg of BBE was chosen for subsequent in vivo studies because the results of this dose response experiment did not show a significant difference in tumor size between those mice treated with 20 mg/kg compared to any of the higher doses. We chose the lowest possible effective dose of BBE to limit the potential for toxicity. Survival studies showed a significant advantage for mice with HE receiving a single daily gavage dose of BBE (20 mg/kg) compared to those receiving only vehicle control as shown by Kaplan–Meier survival curves (Fig. 1B).

Blood oxidative stress indices were measured to determine whether oral BBE administration influenced systemic changes

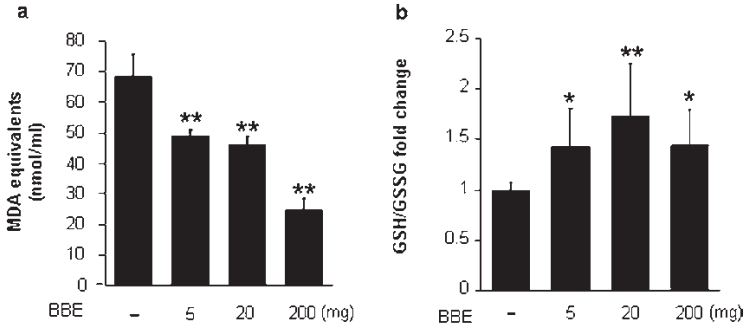

FIG. 2. Oral administration of BBE protects against oxidative events in lipid and aqueous compartments in the blood. Mouse blood was collected at time of necropsy performed 7 days after EOMA cell injection ($n = 6$ mice per treatment group). (**a**) Oxidative end products in the lipid compartment were detected using the TBARS assay. A dose-dependent statistically significant decrease in lipid peroxidation was seen for all doses of BBE treatment compared to vehicle-treated controls (samples run in triplicate ×2; $^{**}p < 0.01$ ANOVA); (**b**) BBE improved serum glutathione redox state (GSH/GSSG). A dose-dependent increase in the ratio of reduced glutathione (GSH) to oxidized glutathione (GSSG) was observed up to a dose of 20 mg/kg of BBE. There was a slight increase in GSH/GGSG ratio observed at the 200 mg/kg dose. The difference in GSH/GSSG ratio was statistically significant for all doses compared to the vehicle treated (ddH_2O) control (mean ± SD; $^{*}p < 0.03$; $^{**}p < 0.01$ ANOVA).

Table 1. Blood GSH and GSSG in Response to BBE Supplementation

BBE dose (mg/kg)	*GSH (pM)*	*GSSG (pM)*	*GSH/GSSG*
0	4052 ± 1650	701 ± 275	5.78 ± 0.88
5	5310 ± 1504	664 ± 271	8.36 ± 1.52
20	5291 ± 1139	404 ± 206	15.13 ± 4.82
200	5313 ± 574	572 ± 93	9.41 ± 1.25

Values are mean ± SD.
BBE, blueberry extract; GSH, reduced glutathione; GSSG, oxidized glutathione.

in the mouse antioxidant capacity. BBE clearly attenuated lipid peroxidation as measured by TBARS (Fig. 2a). Glutathione is the primary cytosolic (aqueous phase) antioxidant in cellular systems. The ratio of reduced versus oxidized glutathione (GSH/GSSG) is frequently used as a measure of oxidative stress, and it was measured in mouse blood using HPLC (Table 1). If BBE was functioning as an antioxidant, then a decrease in the amount of oxidized glutathione should have occurred. The smaller denominator would result in an increased GSH/GSSG ratio. There was a dose-dependent increase in the GSH/GSSG ratio up to the 20 mg/kg dose of BBE, which was not observed at the 200 mg/kg dose (Fig. 2b). Thus, oral BBE administration attenuates oxidative stress indices

A veterinary pathologist performed toxicity studies on mice with HE and treated with gavage feed of either vehicle control or 1,000 mg/kg of BBE. Tissue necropsy was performed on heart, lungs, brain, kidneys, adrenal glands, and skin. Serologic studies evaluating liver and renal function were also performed. There were no differences observed between controls or BBE treated mice for either tissue or serologic studies and all observed serologic results were within the range of normal values for mice without HE (Table 2). An LDH assay was done to make sure the dose of BBE used for *in vitro* assays was not toxic. There was no increase in LDH release from EOMA cells treated with BBE as compared to untreated EOMA cells (Fig. 3). Based upon these results and previously reported evidence of toxicity at 250 μg/ml using propidium iodide exclusion (3), the 150 μg/ml dose of BBE was chosen for the subsequent *in vitro* experiments.

In vitro experiments were performed to gain greater insight into the mechanistic effects of BBE on EOMA cells. Mechanistic studies were not performed on homogenized tumor specimens because the majority of the spongy tumor volume is made of sequestered red blood cells and platelets caused by the Kassabach–Merritt syndrome, not EOMA cells. JNK was chosen for investigation as a potential target for BBE because of its reported potential role in regulating tumor formation. It was important to establish the biologic effects of JNK activation in this endothelial cell neoplasm model because JNK has been shown to have context-dependent tumor suppressor or tumor promoting properties for many different cancers (17, 22, 30).

BBE inhibited TNF-α- induced JNK activation. EOMA cells were pretreated overnight with BBE (150 μg/ml) prior to adding either TNF-α (400 IU/ml) or SP600125 (30 μM), a reversible inhibitor of JNK (16). Phosphorylation of JNK at the threonine 183/tyrosine 185 protein is required for its activation (43). A monoclonal antibody that specifically detects JNK phosphorylated at the threonine 183/tyrosine 185 sites was used. A polyclonal antibody that detects all forms of JNK was used simultaneously on a duplicate set of samples to measure total JNK. Results were normalized by reporting them as a ratio between phosphorylated JNK versus total JNK. TNF-α induced JNK activation was significantly inhibited by pretreatment with BBE (Fig. 4a). Ratios of phosphorylated versus total JNK were 0.5 or less, indicating that at least twice as much total JNK was available as phosphorylated JNK. Thus, substrate availability was not a rate-limiting factor for this reaction.

The ability of BBE to inhibit downstream signaling events as a result of JNK inhibition was also investigated. One function of JNK is to phosphorylate c-Jun at serine 63 and 73 to facilitate the formation of AP-1 (26). The ability of BBE to inhibit c-Jun phosphorylation was measured with an ELISA assay. The primary antibody detects phosphorylation of c-Jun at serine 73 isolated from nuclear extract and bound to a consensus binding site oligonucleotide coated on the bottom of a 96-well plate. EOMA cells were pretreated with BBE and the ability to inhibit TNF-α induced c-Jun activation measured. BBE significantly inhibited TNF-α-induced c-Jun phosphorylation/ activation (Fig. 4B) and binding to AP-1 consensus binding sequences.

The next step in the JNK signaling pathway after c-Jun phosphorylation is binding of c-Jun with c-Fos to form the nuclear transcription factor AP-1. Inhibition of AP-1 bioactivity was detected using a AP-1 reporter assay. BBE treatment of EOMA cells significantly inhibited AP-1 promoter binding (Fig. 4C).

AP-1 is known to regulate inducible MCP-1 expression. AP-1 binds at -68bp in the MCP-1 promoter and overexpression of c-Jun in endothelial cells is known to result in

Table 2. Hepatic and Renal Function Tests in Response to BBE Supplementation

	Liver function (units/liter)				*Renal function (mg/deciliter)*			
	ALT (normal = 14.1–110)		*AST (normal = 49.6–171.2)*		*BUN (normal = 20.9–40.5)*		*Creatinine (normal = 0.41–0.83)*	
BBE dose (mg/kg)	*day 0*	*day 7*	*day 0*	*day 7*	*day 0*	*day 7*	*day 0*	*day 7*
0 (n = 3)	30.7 ± 2.3	22.3 ± 2	100 ± 5.6	121.8 ± 22.1	32 ± 0	22.2 ± 3.2	0.4 ± 0	0.35 ± 0.05
1000 (n = 3)	30.7 ± 6.1	23.1 ± 4.5	156 ± 50	104.9 ± 12.3	28 ± 0	24.3 ± 3.1	0.4 ± 0	0.43 ± 0.18

Values are mean ± SD.
ALT, alanine transaminase; AST, aspartate transaminase; BUN, blood urea nitrogen.

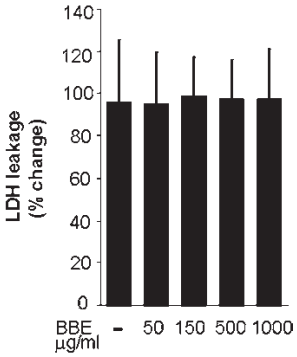

FIG. 3. *In vitro* assays of BBE toxicity. LDH assay to test cell viability showed that the BBE treatment *in vitro* is nontoxic to EOMA cells compared to untreated controls with no difference in the amount of LDH secreted or retained by untreated vs. BBE treated cells. Results are normalized by reporting secreted LDH as a percentage of total LDH (LDH cell sups + LDH cell lysate) for each sample. Samples run in triplicate ×3 (mean ± SD, ANOVA).

MCP-1 expression (34, 57, 63). Since MCP-1 expression has been shown to be required for HE tumor development (14), we sought to determine whether BBE inhibited MCP-1 expression by EOMA cells. This hypothesis was affirmed by ELISA, which showed that TNF-α-inducible MCP-1 protein expression was strongly inhibited by BBE treatment (Fig. 5a). However, the extent of MCP-1 inhibition seemed much more pronounced than the observed effects of BBE on AP-1 inhibition, which suggested that there may have been other stimuli for MCP-1 expression that were BBE sensitive. When the effects of BBE on NF-κB activation in EOMA cells were evaluated, a significant inhibition of both basal as well as TNF-α-inducible NF-κB activation was noted (Fig. 5b). Thus, the strong inhibitory effects of BBE on MCP-1 expression in EOMA cells are the result of diminished signaling via both the NF-κB and JNK signaling pathways.

EOMA cells are endothelial cells that form anastomoses with host vasculature to create a tumor consisting of blood filled vascular spaces. This means that angiogenesis is an inherent process in HE development. The ability of BBE to inhibit angiogenic behavior was tested by examining EOMA cell tube formation on Matrigel, migration in a transwell system, and regulation of cell proliferation. The biological importance of JNK in promoting angiogenesis and HE development and its significance as a potential therapeutic target was also evaluated in these assays using the JNK inhibitor SP600125 as a tool. For the tube formation assays, EOMA cells were pretreated with BBE, trypsinized, and then seeded on Matrigel. Vehicle control, SP600125, and BBE treatments were added to EOMA cells at the time they were seeded on Matrigel. Tube formation was calculated as the area within intact circular rings of EOMA cells and normalized by presenting it as a ratio of EOMA cell enclosed area versus the total surface area of Matrigel within the image (Fig. 6a1–4). Both BBE treatment as well as SP600125-dependent inhibition of JNK significantly attenuated tube formation by EOMA cells (Fig. 6b). The transwell assay was performed by

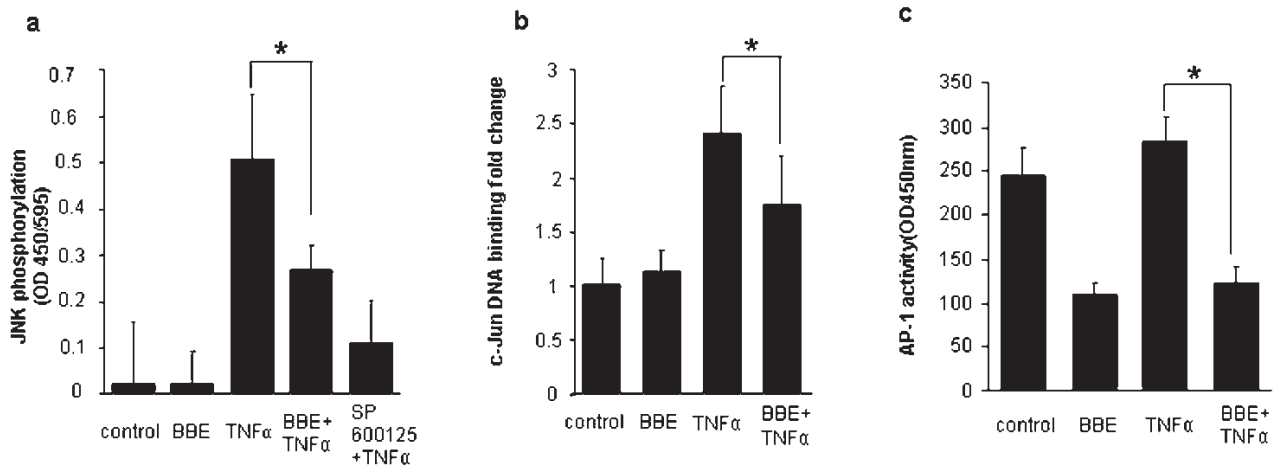

FIG. 4. BBE inhibited JNK signal transduction pathway in EOMA cells. (**a**) EOMA cells were pretreated with BBE (150 μg/ml) for 16 h, and then JNK phosphorylation was either stimulated with TNF-α (400 IU/ml) × 15 min, or inhibited using JNK inhibitor SP600125 (30 μM) × 15 min. JNK phosphorylation was detected using a primary antibody specific for the phosphorylated JNK isoforms and compared to the total amount of JNK available using a different primary antibody to detect all JNK isoforms on a duplicate sample in a separate well. Results for each well were normalized based on relative protein content using a protein stain provided in the kit and measuring absorbance at 595 nm. Results shown in the figure represent the ratio of phosphorylated JNK versus total JNK for each sample. Samples run in triplicate ×2 (mean ± SD; *$p <$ 0.01 ANOVA); (**b**) BBE inhibited cJun phosphorylation. EOMA cells were pretreated with BBE (150 μg/ml) for 16 h and stimulated with TNF-α (400 IU/ml) × 1 h. Nuclear extract from EOMA cells (2 ug/well) were placed in a 96-well plate coated with a consensus oligonucleotide for cJun binding within an AP-1 promoter sequence. A primary antibody was used to detect only phosphorylated c-Jun bound to the consensus oligonucleotide and a secondary HRP-conjugated antibody used for colorimetric measurement. Pretreatment of EOMA cells with BBE significantly inhibited TNF-α induction of c-Jun phosphorylation. Samples were run in triplicate ×2 (mean ± SD; *$p < 0.01$ ANOVA); (**c**) BBE inhibited AP-1 activation. The pAP-1luc plasmid was used to detect binding of AP-1 to transcriptional activation sites contained within the promoter for the firefly luciferase reporter gene. AP-1 binding was detected using a luminometer to quantify luciferase levels Treatment of EOMA cells with BBE (150 μg/ml) for 16 h inhibited AP-1 promoter binding activity compared to both basal levels of expression in untreated cells and cells stimulated with TNF-α (400 IU/ml) × 1 h. Samples were run in quadruplicate ×2 (mean ± SD; *$p < 0.01$, ANOVA).

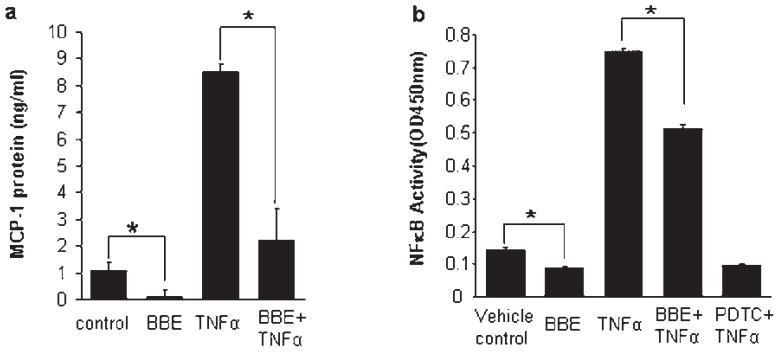

FIG. 5. BBE inhibited MCP-1 protein expression and NF-κB transactivation. (**a**) Pretreatment of EOMA cells with BBE (150 μg/ml) for 16 h significantly inhibited both basal as well as TNF-α (400 IU/ml $\times$ 2 h) inducible MCP-1 protein expression detected by ELISA. Samples were run in triplicate $\times$3 (mean $\pm$ SD; *$p < 0.01$ ANOVA). (**b**) EOMA cells were pretreated for 16 h with BBE (150 μg/ml) and then stimulated with TNF-α (400 IU/ml) for 15 min. Pyrollidine dithiocarbamate (PDTC, 0.2 m*M*), a standard inhibitor of NF-κB, was used as control and added at the same time as the TNF-α. Nuclear extract from EOMA cells (10 μg/well) were placed in a 96-well plate coated with a consensus oligonucleotide for p65 binding. A primary antibody was used to detect p65 bound to the consensus oligonucleotide and a secondary HRP-conjugated antibody used for colorimetric measurement. Pretreatment of EOMA cells with BBE significantly inhibited TNF-α induction of p65/NF-κB nuclear translocation . Samples were run in triplicate $\times$ 2 (mean $\pm$ SD; * $p < 0.01$ ANOVA).

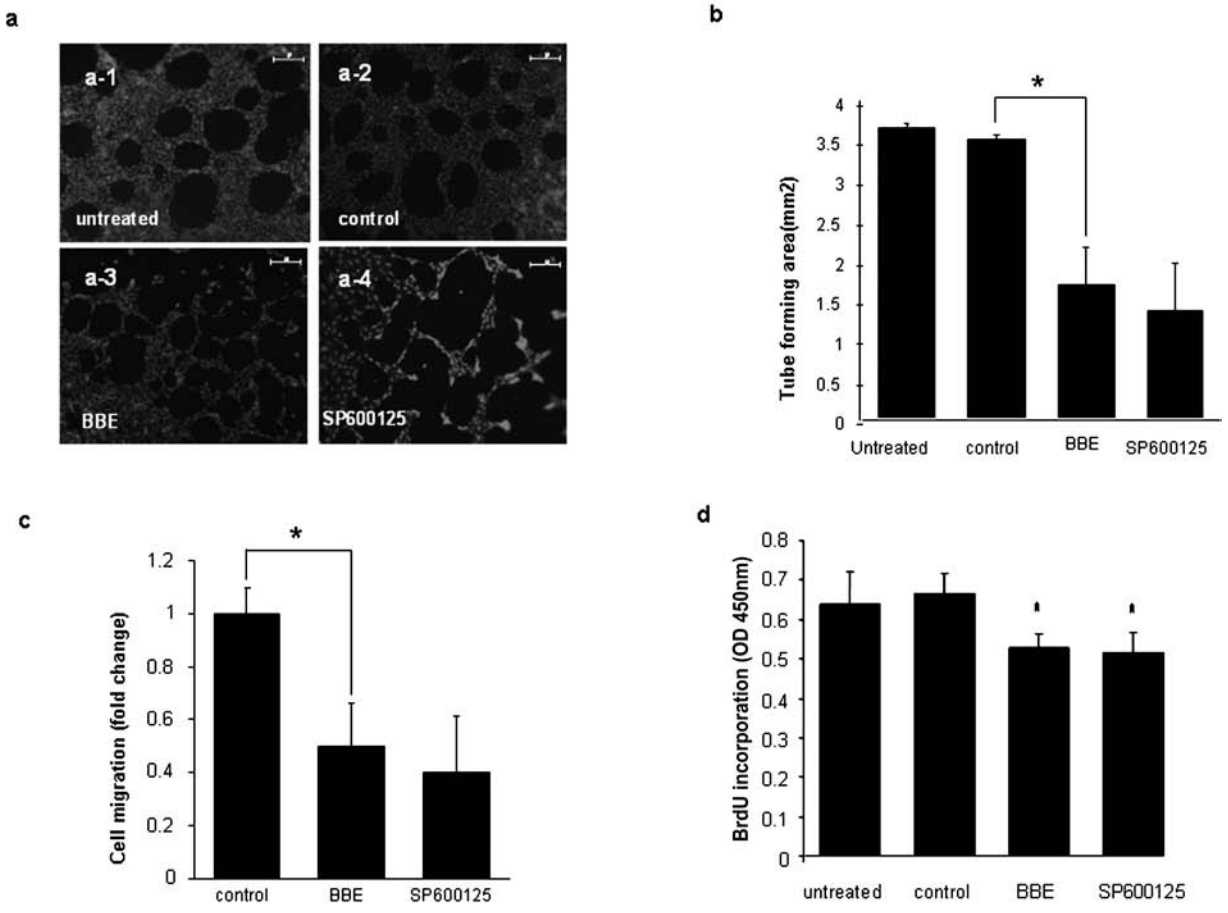

FIG. 6. BBE inhibited the angiogenic activity of EOMA cells. (**a**) EOMA cells grown on Matrigel demonstrate angiogenic behavior/tube formation which is inhibited by treatment with BBE (150 μg/ml) or JNK inhibitor SP600125 (30 μ*M*). Imaging of EOMA cells grown on Matrigel was done using calcein AM and DAPI was used to label nuclei. (**a-1**) untreated, (**a-2**) vehicle control, (**a-3**) BBE treatment (150 μg/ml), (**a-4**) SP600125 (30 μ*M*) (a-d scale bar = 200 μm), **(b)** Tube formation on Matrigel was quantified using the AxioVision software. * $p < 0.01$; **(c)** BBE inhibited EOMA cell migration. EOMA cells cultured in LSM (0.5% FBS), treated with BBE (150 μg/ml) and placed in the upper chamber of a transwell system showed decreased migration toward the lower chamber compared to cells in the same conditions treated with vehicle control (0.3% DMSO). Cell migration was also inhibited by treatment with the JNK inhibitor SP600125 (30 μM). Lower chambers were filled with NGM, which contains a higher serum content (10% FBS), than the LSM. No cells were placed in the lower chambers. There were 6 samples per treatment group with 3 cell migration measurements per sample *$p < 0.01$ ANOVA. (**d**) BrdU assay showed a significant decrease in the rate of EOMA cell proliferation with BBE treatment (150 μg/ml) compared to vehicle treated cells. A significant difference was also seen when treating cells with JNK inhibitor SP600125 (30 μM) suggesting that the observed effects of BBE on cell proliferation may be mediated through JNK. Samples run in triplicate $\times$ 3 (mean $\pm$ SD *$p < 0.01$, ANOVA)

placing EOMA cells in the upper chamber in LSM (0.5% FCS) and filling the lower chamber with NGM (10% FCS) to create a serum gradient as a stimulus for migration. No cells were placed in the lower chambers. EOMA cell migration was significantly inhibited by treatment with BBE or the JNK inhibitor SP600125 compared to vehicle treated controls (Fig. 6C). Both BBE treatment, as well as JNK inhibition, decreased EOMA cell migration. Thus, JNK inhibition is a biologically relevant target for this endothelial cell neoplasm and the ability of BBE to inhibit EOMA cell angiogenic responses may be mediated by its inhibitory effects on JNK activation. As a measure of cell proliferation, BrdU incorporation was compared between untreated EOMA cells and those treated with BBE or SP600125. Specific inhibition of JNK activation with SP600125 clearly inhibited EOMA cell proliferation. Consistent results demonstrating significant inhibition of EOMA cell proliferation was noted in response to BBE treatment (Fig. 6D).

Discusssion

The general purpose of these investigations was two-fold: (a) determine whether oral administration of BBE had any impact on endothelial cell tumor growth *in vivo*, and (b) identify the mechanisms by which BBE exerts its effects. Results of this study show that oral administration of blueberry extract can inhibit the growth of endothelial neoplasms *in vivo* and enhance survival. No toxicity was observed at doses 50 times greater than that necessary to achieve a clinically significant impact on survival and tumor size, which reinforces the safety of using a nutritional approach and also provides a large window to explore for potential dosing.

Blueberry extract (BBE) is rich in anthocyanins, which possess potent antioxidant properties that may contribute to their antineoplastic effects (25, 44). Documenting a systemic change in the blood redox status in response to BBE treatment was significant for two reasons. First, the NF-κB and JNK signaling pathways that were identified in mediating the effects of BBE are known to be redox sensitive (7, 33, 40, 58). Second, we have previously demonstrated that MCP-1 expression in EOMA cells is decreased in the presence of antioxidants (15) .

This is the first report to demonstrate that blueberry extract specifically inhibits the JNK signaling pathway. JNK was selected as a potential target because one of the flavonoid components present in blueberry extract, epigallocatechin 3-gallate (ECGC), can activate transcription of the tumor suppressor gene $p21^{WAF1/CIP1}$ independent of p53, which forms a tight complex with JNK-1 to inactivate it (42, 55). The outcome of JNK-1 activity is phosphorylation/activation of c-Jun and constituent activation of c-Jun in endothelial cells has been shown to result in MCP-1 expression (62). The *in vitro* effects of BBE and JNK inhibition observed in the EOMA model are consistent with other published reports. JNK has been shown to promote proliferation in other cell lines, including human A549 lung carcinoma cells, multiple myeloma cells, and breast cancer cells (5, 19, 35). JNK has also been shown in endothelial cells to inhibit proliferation, migration, and the angiogenic pattern of endothelial cell sprouting on Matrigel (56). Results of this study showed that BBE treatment or specific inhibition of JNK decreased EOMA cell proliferation, migration, and tube formation on Matrigel, that are all important indicators for potential tumor growth *in vivo*.

The results achieved with oral administration of BBE in the EOMA model are consistent with other reports at *in vivo* attempts to inhibit tumor growth through JNK inhibition. A statistically significant drop in tumor volume was seen in SCID mice bearing tumors derived from DU145 prostate carcinoma cell line that were treated with once daily with intraperitoneal injections of SP600125 (12). In another case, complete inhibition of intestinal tumor formation was achieved when c-Jun was completely eliminated from the intestinal epithelium using a conditional c-Jun knockout model(36). These observations suggest that inhibiting JNK activity may be an effective strategy for treating tumors with a direct correlation between the extent of JNK inhibition and the impact on tumor growth. Whereas there was a statistically significant reduction in tumor volume with once daily dosing of BBE, it is unlikely that maximal benefit was achieved with this dosing regimen. The fact that we have previously demonstrated that the incidence of tumor formation and tumor size could be significantly decreased by delivering BBE to EOMA cells *in vitro* prior to injection, suggests that greater clinical efficacy may be achieved by optimizing the ability of BBE to reach EOMA cell *in vivo* (3).

Demonstrating the effects of BBE on AP-1 was significant because AP-1 has been shown to play a critical role in tumor development (9, 32). Specifically, increased AP-1 activity is involved in the tumor promotion and progression phases of carcinogenesis both *in vitro* and *in vivo* (6, 10, 11, 45, 49, 66). Anthocyanins, which are plentiful in blueberries, have specifically been shown to inhibit AP-1 activity and the transformation process (8, 21). Results from reporter studies show that EOMA cells have a very high level of basal AP-1 activity consistent with the transformed status of the cell line. The inhibition of AP-1 binding activity observed with BBE treatment may be attributable to BBE limiting the availability of activated/phosphorylated c-Jun necessary for AP-1 formation and promoter binding.

Finally, the critical role of MCP-1 in this model and the ability of BBE to inhibit its expression cannot be overstated. The role of macrophages in promoting tumor growth is gaining wider recognition (4, 31, 52) , and we have previously demonstrated that HE fail to develop in the absence of MCP-1 and macrophages (14). The fact that MCP-1 expression is limited to the proliferative phase of growth for the most common form of endothelial cell neoplasm (infantile hemangiomas have both proliferative and involutional phases) combined with its required role in HE tumor development make it an important therapeutic target. The expression of MCP-1 in other tumors and its established correlation with outcomes in breast cancer reinforces this notion. The results presented herein show that BBE can inhibit key therapeutic targets, including MCP-1 protein expression. BBE can also achieve clinically significant results when given orally in a treatment scenario that is consistent with what occurs in the clinical setting.

A nutritional intervention for endothelial neoplasms has many potential benefits. Infants could be treated at the first signs that the lesion is present and hopefully avoid the need for higher risk treatment options and the potential for deformity altogether. It also makes treatment available to patients that have an obvious physical deformity, but no other

risks related to the lesion. Alternatively, it could be considered as a possible adjunctive therapy for steroids or interferon to try and shorten the length of treatment, which usually lasts for at least 6 months, or the maximum dose required to achieve tumor regression. There has been one clinical case in which BBE was effective in treating a teenage girl with diffuse hemangiomatosis and life-threatening Kassabach–Merrit phenomenon resistant to steroid therapy (Konrad K. Siala, Prague, Czechoslovakia, personal communication). Thus, BBE has the potential to replace or enhance steroid therapy. Given these results and the potential benefits of a nutritional approach, BBE merits further consideration for possible clinical trials.

Acknowledgments

Funding for this work is supported by the NIH/NIGMS K08GM066964 (GMG). The work was also supported in part by GM069589 to CKS.

Abbreviations

AP-1, activator protein-1; BBE, blueberry extract; BrdU, bromodeoxyuridine; ddH_2O, double distilled water; DMSO, dimethyl sulfoxide; GSH, reduced glutathione; GSSG, oxidized glutathione; HE, hemangioendothelioma; HPLC, high pressure liquid chromatography; IU, international units; JNK, c-Jun N-terminal kinase; LDH, lactate dehydrogenase; LSM, low serum media; MCP-1, monocyte chemoattractant protein-1; MDA, malondialdehyde; NF-kB, nuclear factor-kappaB; NGM, normal growth media; PDTC, pyrollidine dithiocarbamate; TBARS, thiobarbituric acid reactive substances; TNF-α, tumor necrosis factor-alpha.

References

1. Albini A, Morini M, D'Agostini F, Ferrari N, Campelli F, Arena G, Noonan DM, Pesce C, and De Flora S. Inhibition of angiogenesis-driven Kaposi's sarcoma tumor growth in nude mice by oral N-acetylcysteine. *Cancer Res* 61: 8171–8178, 2001.
2. Amann B, Pearbo F, Wirger A, Hugenschmidt H, and Schultze–Seeman W. Urinaryl levels of monocyte chemoattractant protein-1 correlate with tumor stage and grade in patients wih bladder cancer. *Br J Urol* 82: 118–121, 1998.
3. Atalay M, Gordillo G, Roy S, Rovin B, Bagchi D, Bagchi M, and Sen CK. Anti-angiogenic property of edible berry in a model of hemangioma. *FEBS Lett* 544: 252–257, 2003.
4. Biswas SK, Sica A, and Lewis CE. Plasticity of macrophage function during tumor progression: regulation by distinct molecular mechanisms. *J Immunol* 180: 2011–2017, 2008.
5. Bost F, McKay R, Bost M, Potapova O, Dean NM, and Mercola D. The Jun kinase 2 isoform is preferentially required for epidermal growth factor-induced transformation of human A549 lung carcinoma cells. *Molecular and cellular biology* 19: 1938-1949, 1999.
6. Chen N, Nomura M, She QB, Ma WY, Bode AM, Wang L, Flavell RA, and Dong Z. Suppression of skin tumorigenesis in c-Jun NH(2)-terminal kinase-2-deficient mice. *Cancer Res* 61: 3908–3912, 2001.
7. Chen YR, Wang W, Kong AN, and Tan TH. Molecular mechanisms of c-Jun N-terminal kinase-mediated apoptosis induced by anticarcinogenic isothiocyanates. *J Biol Chem* 273: 1769–1775, 1998.
8. Ding M, Lu Y, Bowman L, Huang C, Leonard S, Wang L, Vallyathan V, Castranova V, and Shi X. Inhibition of AP-1 and neoplastic transformation by fresh apple peel extract. *J Biol Chem* 279: 10670–10676, 2004.
9. Dong Z, Birrer MJ, Watts RG, Matrisian LM, and Colburn NH. Blocking of tumor promoter-induced AP-1 activity inhibits induced transformation in JB6 mouse epidermal cells. *Proc Nat Acad Sci USA* 91: 609–613, 1994.
10. Dong Z, Crawford HC, Lavrovsky V, Taub D, Watts R, Matrisian LM, and Colburn NH. A dominant negative mutant of jun blocking 12-O-tetradecanoylphorbol-13-acetate-induced invasion in mouse keratinocytes. *Mol Carcinogen* 19: 204–212, 1997.
11. Dumont JA, Bitonti AJ, Wallace CD, Baumann RJ, Cashman EA, and Cross-Doersen DE. Progression of MCF-7 breast cancer cells to antiestrogen-resistant phenotype is accompanied by elevated levels of AP-1 DNA-binding activity. *Cell Growth Diff* 7: 351–359, 1996.
12. Ennis BW, Fultz KE, Smith KA, Westwick JK, Zhu D, Boluro–Ajayi M, Bilter GK, and Stein B. Inhibition of tumor growth, angiogenesis, and tumor cell proliferation by a small molecule inhibitor of c-Jun N-terminal kinase. *J Pharmacol Exp Ther* 313: 325–332, 2005.
13. Folkman J, Mulliken J, and Ezekowitz R. Angiogenesis and hemangiomas. In: *Surgery of Infants and Children: Scientific Principles and Practice*, edited by Oldham K. Philadelphia: Lippincott–Raven, 1997, p. 569–584.
14. Gordillo G, Onat D, Stockinger M, Roy S, Atalay M, Beck M, and Sen C. A key angiogenic role of monocyte chemoattractant protein-1 in hemangioendothelioma proliferation. *Am J Physiol (Cell)* 287: C866–873, 2004.
15. Gordillo GM, Atalay M, Roy S, and Sen CK. Hemangioma model for in vivo angiogenesis: inducible oxidative stress and MCP-1 expression in EOMA cells. *Methods Enzymol* 352: 422–432, 2002.
16. Harper S and LoGrasso P. Inhibitors of JNK signaling pathway. *Drugs of the Future* 26: 957–973, 2001.
17. Heasley LE and Han S–Y. JNK regulation of oncogenesis. *Mol Cells* 21: 167–173, 2006.
18. Hefler L, Tempfer C, Heinze G, Mayerhofer K, Breitenecker G, Leodolter S, Reinthaller A, and Kainz C. Monocyte chemoattractant protein-1 serum levels in ovarian cancer patients. *Br J Cancer* 81: 855–859, 1999.
19. Hideshima T, Hayashi T, Chauhan D, Akiyama M, Richardson P, and Anderson K. Biologic sequelae of c-Jun NH(2)-terminal kinase (JNK) activation in multiple myeloma cell lines. *Oncogene* 22: 8797–8801, 2003.
20. Hoak JC, Warner ED, Cheng HF, Fry GL, and Hankenson RR. Hemangioma with thrombocytopenia and microangiopathic anemia (Kasabach–Merritt syndrome): an animal model. *J Lab Clin Med* 77: 941–950, 1971.
21. Hou DX, Kai K, Li JJ, Lin S, Terahara N, Wakamatsu M, Fujii M, Young MR, and Colburn N. Anthocyanidins inhibit activator protein 1 activity and cell transformation: structure-activity relationship and molecular mechanisms. *Carcinogenesis* 25: 29–36, 2004.
22. Ichijo H. From receptors to stress-activated MAP kinases. *Oncogene* 18: 6087–6093, 1999.
23. Isik F, Rand R, Gruss J, Benjamin D, and Alpers C. Monocyte chemoattractant protein-1 mRNA expression in hemangiomas and vascular malformations. *J Surg Res* 61: 71–76, 1996.
24. Jang M, Cai L, Udeani GO, Slowing KV, Thomas CF, Beecher CW, Fong HH, Farnsworth NR, Kinghorn AD, Mehta RG, Moon RC, and Pezzuto JM. Cancer chemopreventive activ-

ity of resveratrol, a natural product derived from grapes. *Science New York* 275: 218–220, 1997.
25. Kahkonen MP, Hopia AI, and Heinonen M. Berry phenolics and their antioxidant activity. *J Agric Food Chem* 49: 4076–4082, 2001.
26. Karin M. The regulation of AP-1 activity by mitogen-activated protein kinases. *J Biol Chem* 270: 16483–16486, 1995.
27. Koyama J, Morita I, Kobayashi N, Konoshima T, Takasaki M, Osakai T, and Tokuda H. Correlation between oxidation potentials and inhibitory effects on Epstein–Barr virus activation of flavonoids. *Cancer Lett* 263: 61–66, 2008.
28. Lannutti B, Gately S, Quevedo M, Soff G, and Paller A. Human angiostatin inhibits murine hemangioendothelioma tumor growth *in vivo*. *Cancer Res* 57: 5277-5280, 1997.
29. Leek RD, Lewis CE, Whitehouse R, Greenall M, Clarke J, and Harris AL. Association of macrophage infiltration with angiogenesis and prognosis in invasive breast carcinoma. *Cancer Res* 56: 4625–4629, 1996.
30. Leppa S and Bohmann D. Diverse functions of JNK signaling and c-Jun in stress response and apoptosis. *Oncogene* 18: 6158–6162, 1999.
31. Lewis CE, De Palma M, and Naldini L. Tie2-expressing monocytes and tumor angiogenesis: regulation by hypoxia and angiopoietin-2. *Cancer Res* 67: 8429–8432, 2007.
32. Li JJ, Dong Z, Dawson MI, and Colburn NH. Inhibition of tumor promoter-induced transformation by retinoids that transrepress AP-1 without transactivating retinoic acid response element. *Cancer Res* 56: 483–489, 1996.
33. Lo YY, Wong JM, and Cruz TF. Reactive oxygen species mediate cytokine activation of c-Jun NH2-terminal kinases. *J Biol Chem* 271: 15703–15707, 1996.
34. Martin T, Cardelli P, Parry G, Felts K, and Cobb R. Cytokine induction of monocyte chemoattractant protein-1 gene expression in human endothelial cells depends upon the cooperative action of NF-kappaB and AP-1. *Eur J Immunol* 27: 1091–1097, 1997.
35. Mingo–Sion AM, Marietta PM, Koller E, Wolf DM, and Van Den Berg CL. Inhibition of JNK reduces G2/M transit independent of p53, leading to endoreduplication, decreased proliferation, and apoptosis in breast cancer cells. *Oncogene* 23: 596–604, 2004.
36. Nateri AS, Spencer–Dene B, and Behrens A. Interaction of phosphorylated c-Jun with TCF4 regulates intestinal cancer development. *Nature* 437: 281–285, 2005.
37. O'Reilly M, Brem H, and Folkman J. Treatment of murine hemangioendotheliomas with the angiogenesis inhibitor AGM-1470. *J Ped Surg* 30: 325–330, 1995.
38. Obeso J, Weber J, and Auerbach R. A hemangioendothelioma-derived cell line: its use as a model for the study of endothelial cell biology. *Lab Invest* 63: 259–269, 1990.
39. Paller AS. Responses to anti-angiogenic therapies. *J Invest Dermatol Symp Proc* 5: 83–86, 2000.
40. Park HS, Park E, Kim MS, Ahn K, Kim IY, and Choi EJ. Selenite inhibits the c-Jun N-terminal kinase/stress-activated protein kinase (JNK/SAPK) through a thiol redox mechanism. *J Biol Chem* 275: 2527–2531, 2000.
41. Pataki T, Bak I, Kovacs P, Bagchi D, Das DK, and Tosaki A. Grape seed proanthocyanidins improved cardiac recovery during reperfusion after ischemia in isolated rat hearts. *Am J Clin Nut* 75: 894–899, 2002.
42. Patel R, Bartosch B, and Blank JL. p21WAF1 is dynamically associated with JNK in human T-lymphocytes during cell cycle progression. *J Cell Sci* 111: 2247–2255, 1998.
43. Payne DM, Rossomando AJ, Martino P, Erickson AK, Her JH, Shabanowitz J, Hunt DF, Weber MJ, and Sturgill TW. Identification of the regulatory phosphorylation sites in pp42/mitogen-activated protein kinase (MAP kinase). *EMBO J* 10: 885–892, 1991.
44. Pool–Zobel BL, Bub A, Schroder N, and Rechkemmer G. Anthocyanins are potent antioxidants in model systems but do not reduce endogenous oxidative DNA damage in human colon cells. *Eur J Nut* 38: 227–234, 1999.
45. Risse–Hackl G, Adamkiewicz J, Wimmel A, and Schuermann M. Transition from SCLC to NSCLC phenotype is accompanied by an increased TRE-binding activity and recruitment of specific AP-1 proteins. *Oncogene* 16: 3057–3068, 1998.
46. Rogerio AP, Kanashiro A, Fontanari C, da Silva EV, Lucisano–Valim YM, Soares EG, and Faccioli LH. Anti-inflammatory activity of quercetin and isoquercitrin in experimental murine allergic asthma. *Inflamm Res* 56: 402–408, 2007.
47. Roy S, Khanna S, Alessio HM, Vider J, Bagchi D, Bagchi M, and Sen CK. Anti-angiogenic property of edible berries. *Free Rad Res* 36: 1023–1031, 2002.
48. Roy S, Venojarvi M, Khanna S, and Sen CK. Simultaneous detection of tocopherols and tocotrienols in biological samples using HPLC-coulometric electrode array. *Methods Enzymol* 352: 326–332, 2002.
49. Saez E, Rutberg SE, Mueller E, Oppenheim H, Smoluk J, Yuspa SH, and Spiegelman BM. c-fos is required for malignant progression of skin tumors. *Cell* 82: 721–732, 1995.
50. Sage H and Bornstein P. Endothelial cells from umbilical vein and hemangioendothelioma secrete basement mebrane largely to the exclusion of interstitial procollagens. *Arteriosclerosis* 2: 27–36, 1982.
51. Saji H, Koike M, Yamori T, Saji S, Seiki M, Matsushima K, and Toi M. Significant correlation of monocyte chemoattractant protein-1 expression with neovascularization and progression of breast carcinoma. *Cancer* 92: 1085–1091, 2001.
52. Semenza GL. A new weapon for attacking tumor blood vessels. *New Eng J Med* 358: 2066–2067, 2008.
53. Sen CK, Khanna S, Roy S, and Packer L. Molecular basis of vitamin E action. Tocotrienol potently inhibits glutamate-induced pp60(c-Src) kinase activation and death of HT4 neuronal cells. *J Biol Chem* 275: 13049–13055, 2000.
54. Serafini M, Laranjinha JA, Almeida LM, and Maiani G. Inhibition of human LDL lipid peroxidation by phenol-rich beverages and their impact on plasma total antioxidant capacity in humans. *J Nutr Biochem* 11: 585–590, 2000.
55. Shim J, Lee H, Park J, Kim H, and Choi EJ. A non-enzymatic p21 protein inhibitor of stress-activated protein kinases. *Nature* 381: 804–806, 1996.
56. Shin EY, Kim SY, and Kim EG. c-Jun N-terminal kinase is involved in motility of endothelial cell. *Exp Mol Med* 33: 276–283, 2001.
57. Sica A, Wang J, Collota F, DeJana E, Montovani A, Larsen C, Zachariae C, and Matsushima K. Monocyte chemotactic and activating factor gene expression induced in endothelial cells by IL-1 and tumor necrosis factor. *J Immunol* 144: 3034–3038, 1990.
58. Surh YJ, Kundu JK, Na HK, and Lee JS. Redox-sensitive transcription factors as prime targets for chemoprevention with anti-inflammatory and antioxidative phytochemicals. *J Nutr* 135: 2993S–3001S, 2005.
59. Szabo ME, Gallyas E, Bak I, Rakotovao A, Boucher F, de Leiris J, Nagy N, Varga E, and Tosaki A. Heme oxygenase-1-related carbon monoxide and flavonoids in ischemic/reperfused rat retina. *Invest Ophthalmol Vis Sci* 45: 3727–3732, 2004.

60. Taraboletti G, Garofalo A, Belotti D, Drudis T, Borsotti P, Scanziani E, Brown PD, and Giavazzi R. Inhibition of angiogenesis and murine hemangioma growth by batimastat, a synthetic inhibitor of matrix metalloproteinases. *J Nat Cancer Inst* 87: 293–298, 1995.
61. Ueno T, Toi M, Saji H, Muta M, Bando H, Kuroi K, Koike M, Inadera H, and Matsushima K. Significance of macrophage chemoattractant protein-1 in macrophage recruitment, angiogenesis, and survival in human breast cancer. *Clin Cancer Res* 6: 3282–3289, 2000.
62. Wang C, Quevedo ME, Lannutti BJ, Gordon KB, Guo D, Sun W, and Paller AS. In vivo gene therapy with interleukin-12 inhibits primary vascular tumor growth and induces apoptosis in a mouse model. *J Invest Dermatol* 112: 775–781, 1999.
63. Wang N, Verna L, Hardy S, Forsayeth J, Zhu Y, and Stemerman MB. Adenovirus-mediated overexpression of c-Jun and c-Fos induces intercellular adhesion molecule-1 and monocyte chemoattractant protein-1 in human endothelial cells. *Arterioscler Thromb Vasc Biol* 19: 2078–2084, 1999.
64. Warner ED, Hoak JC, and Fry GL. Hemangioma, thrombocytopenia, and anemia. The Kasabach–Merritt syndrome in an animal model. *Arch Pathol* 91: 523–528, 1971.
65. Yamamoto Y and Gaynor RB. Therapeutic potential of inhibition of the NF-kappaB pathway in the treatment of inflammation and cancer. *J Clinl Invest* 107: 135–142, 2001.
66. Young MR, Li JJ, Rincon M, Flavell RA, Sathyanarayana BK, Hunziker R, and Colburn N. Transgenic mice demonstrate AP-1 (activator protein-1) transactivation is required for tumor promotion. *Proc Nat Acad Sci USA* 96: 9827–9832, 1999.

Address reprint requests to:
Gayle Gordillo, M.D.
410 W. 10th Avenue
Doan Halll N-809
Columbus, Ohio 43210

E-mail: gayle.gordillo@osumc.edu

Date of first submission to ARS Central, June 9, 2008; date of final revised submission, July 18, 2008; date of acceptance, July 24, 2008.